Statistical Tropical Cyclone Wind Radii Prediction Using Climatology and Persistence: Updates for the Western North Pacific

JOHN A. KNAFF

NOAA/Center for Satellite Applications and Research, Fort Collins, Colorado

CHARLES R. SAMPSON

Naval Research Laboratory, Monterey, California

KATE D. MUSGRAVE

Cooperative Institute for Research in the Atmosphere, Fort Collins, Colorado

(Manuscript received 13 February 2018, in final form 21 June 2018)

ABSTRACT

This note describes an updated tropical cyclone vortex climatology for the western North Pacific version of the operational wind radii climatology and persistence (i.e., CLIPER) model. The update addresses known shortcomings of the existing formulation, namely, that the wind radii used to develop the original model were too small and symmetric. The underlying formulation of the CLIPER model has not changed, but the larger and more realistic vortex climatology produces improved forecast biases. Other applications that make use of the vortex climatology and CLIPER model forecasts should also benefit from the bias improvements.

1. Introduction

The U.S. tropical cyclone (TC) warning centers provide information about TC surface wind structure—analyzed and forecasted in terms of wind radii. The collective term wind radii refers to the maximum radial extent of TC winds exceeding three critical wind speed thresholds in compass quadrants about the storm center: northeast, southeast, southwest, and northwest. The critical wind speed thresholds used at the centers are 34, 50, and 64 kt (1 kt $\approx$ 0.514 m s^{-1}), and are referred to in this paper as R34, R50, and R64, respectively. The U.S. TC warning centers also report and forecast their wind radii in units of nautical miles (1 n mi = 1.85 km), and so we use the units knots and nautical miles throughout this work.

Prior to 2005, forecast guidance for wind radii was considered to be unskillful and of marginal use in operations (Knaff et al. 2007a). Around that time, a simple statistical wind radii forecast guidance based on climatology and persistence (CLIPER) was developed (Knaff et al. 2007b, hereafter K07). The development of this "wind radii CLIPER model" or "DRCL" [the four-letter technique name in the Automated Tropical Cyclone Forecast (ATCF) system; Sampson and Schrader 2000] was part of a larger effort to provide probabilistic forecast information for wind speeds associated with TCs in the North Atlantic and North Pacific (DeMaria et al. 2009, 2013). At that time, the developers were confident that satellite-based ocean wind vectors influenced wind radii estimation and best tracking, as indicated in the following statement in K07:

> During this period, operational centers used several satellite-derived products (low-level atmospheric motion vectors, passive microwave, and scatterometry) in their wind radii estimates. We do not consider these data to be as accurate as the data influenced by aircraft reconnaissance; nevertheless, we use these wind radii datasets and accept their inherent shortcomings.

While this turned out to be true in the basins where the National Hurricane Center (NHC) and Central Pacific

Corresponding author: John Knaff, john.knaff@noaa.gov

DOI: 10.1175/WAF-D-18-0027.1

Hurricane Center (CPHC) had responsibility, this was not the case in the western North Pacific. In hindsight, the western North Pacific wind radii in the best tracks[1] were based on very few observations, mostly fortuitous scatterometer winds and surface observations that were available just prior to the forecaster's real-time estimates. The resulting DRCL model derived for the western North Pacific, which used those real-time estimates, used a climatological vortex that was too small and symmetric. In this note, we describe how three years of objective wind radii best tracks, which closely match subjectively determined wind radii best tracks described in Sampson et al. (2017), are used to rederive the DRCL model used in the western North Pacific. The model updates described in this note are now in operations at the Joint Typhoon Warning Center (JTWC) and serve as both guidance and the skill baseline for TC wind radii forecasts in the western North Pacific.

This update contains a brief summary of the data and methods used for model rederivation, noting that the methods have not changed from K07. We then provide coefficients derived for the new version of DRCL and examine how these differ from the coefficients in the original K07 version. This is followed by a discussion of how the new DRCL formulation works, how it differs from the older version of the model, and its potential impact on operations at JTWC.

2. Data and model update

a. Updated climatology

Three years, 2014–16, of objectively estimated wind radii best tracks were used as input data for creating a climatological dataset. The objective wind radii best track procedures and verification versus a subjectively determined best track are discussed in Sampson et al. (2017). The focus of Sampson et al. (2017) was on 34-kt wind radii estimation in operations. These estimates made use of the available wind radii estimates and helped forecasters more efficiently, systematically, and accurately estimate real-time 34-kt wind radii. An equally weighted mean (or consensus) of real-time objectively determined 34-kt wind radii estimates created a $t = 0$ estimate of wind radii. The inputs to the $t = 0$ consensus included wind radii based on routine Dvorak fixes and matching imagery (i.e., Knaff et al. 2016), microwave sounders (i.e., Demuth et al. 2006), the NESDIS multisatellite-platform surface wind analysis–based fix (Knaff et al. 2011), and 6-h forecasts of wind radii from the Global Forecast System, the Hurricane Weather Research and Forecasting Model, and the Geophysical Fluid Dynamics Laboratory hurricane model. Sampson et al. (2017) created a 2-yr (2014–15) 34-kt wind radii objective analysis using this method. These objective estimates were shown to compare favorably to independently analyzed wind radii estimates contained in the National Hurricane Center's postseason estimates (i.e., the best tracks) and a specially created subjectively analyzed best track dataset for the western North Pacific. In K07 the average west Pacific R34 was 115 n mi, while in Sampson et al. (2017) the postseason analyzed R34 was 134 n mi.

The method used here is the same as in K07 and starts with a generalized version of the modified Rankine vortex that includes a wavenumber one asymmetry [see (1) below]. The wind V is a function of radius r and azimuth θ, and x is the shape parameter, a is the asymmetry, θ_o is the azimuthal orientation, v_m is the maximum wind in the vortex, and r_m is the radius of maximum wind:

$$V(r,\theta) = (v_m - a)\left(\frac{r_m}{r}\right)^x + a\cos(\theta - \theta_o), \quad \text{for} \quad r \geq r_m,$$

$$V(r,\theta) = (v_m - a)\left(\frac{r}{r_m}\right) + a\cos(\theta - \theta_o), \quad \text{for} \quad r < r_m. \tag{1}$$

The four free parameters (i.e., x, a, θ_o, and r_m) in (1) are climatological values of parameters found in the best track (latitude, storm translational speed, and storm maximum winds) as shown in (2). The climatological values are all denoted with the subscript c, and t_0–t_2, a_0–a_3, x_0–x_2, and m_0–m_2 are all constants:

$$\left\{\begin{array}{l} \theta_{oc} = t_0 + t_1\gamma + t_2 c \\ a_c = a_0 + a_1 c + a_2 c^2 + a_3\gamma \\ x_c = x_0 + x_1 v_m + x_2\gamma \\ r_{mc} = m_0 + m_1 v_m + m_2\gamma \end{array}\right\}, \quad \text{where}$$

$$\left\{\begin{array}{l} \gamma \equiv \text{latitude} - 25^\circ \\ c \equiv \text{storm speed} \\ v_m \equiv \text{maximum wind} \end{array}\right\}. \tag{2}$$

The choice of this functional form approximates known variations in tropical cyclone structure. Azimuthal orientation of asymmetries can be affected by interaction with the background environment and here is a function of latitude and translation speed c. Asymmetries are prescribed to be a function of translational speed and

[1] Although wind radii dating back to 1996 can be found in the western North Pacific best tracks, they had not been analyzed postseason until just recently and only for the years 2013–16 (E. Fukada 2017, personal communication).

latitude; the justification of which is discussed by Uhlhorn et al. (2014) and Klotz and Jiang (2016). Tropical cyclone size, which is represented by the shape parameter x, is both a function of intensity (TCs grow larger as they become more intense) and latitude [TCs grow larger as they move poleward; see Knaff et al. (2014), Merrill (1984), and Weatherford and Gray (1988)]. Finally, r_{mc} in (2) is a function of latitude and intensity, following Knaff et al. (2015) and references therein. Allowing r_{mc} to vary with latitude and intensity provides even more variability in the model. For instance, wind radii can be increased simply by assigning a larger value of r_{mc} . One shortcoming of this added variability is that the r_{mc} values are typically unrealistically large when compared to observed radii of maximum wind.

The parametric vortex defined in (1) and (2) has 13 free parameters, and there is no unique set of 13 parameters that would fit a single set of wind radii values in the best track. Instead, the 13 parameters are chosen to minimize the RMS errors of the observed R34, R50, and R64 from a large sample of cases. Because the vortex profile is a nonlinear function of the parameters, there are probably local minima in the RMS error function. It is also likely that some values of the parameters can lead to solutions that are not physically realistic, so penalty terms are employed in the error function to restrict the solutions to physically realistic values. This process is similar to the method of steepest descent first published by Debye (1909). In our algorithm, only one parameter at a time is varied over a range of physically realistic values to avoid the need for a closed form of the gradient of the error function with respect to the 13 parameters. The details of this methodology follow.

Input and output variables in (2) are scaled so that they are of order one. This scaling strategy is the more elegant of the two methods discussed in K07. The scaling factors used were 30 kt, 1, 100 n mi, and 90° for a_c, x_c, r_{mc}, and θ_{oc}, and 165 kt, 50°, and 30 kt for v_m, γ, and c, which are based on near-maximum values in the best tracks. Because we use this scaling, the search increment for each variable is comparable to the other variables. As previously mentioned, vortex parameters are physically constrained by applying a penalty term to the error function (i.e., the RMS difference between the estimated and observed radii). The penalty term increases the RMSE for these cases by multiplying the amount the vortex parameters are out of range by a large coefficient (10^6). The RMSEs with the penalty term act as a loss function, for which we seek a minimum. This method allows the searching algorithm to consider coefficients where vortex parameters are out of range for a few cases, but results in vortex parameters that do not violate physical constraints. For instance, values of $x > 1.0$ (negative absolute vorticity) or $a < 0.0$ (maximum winds stronger than v_m) are not allowed.

The iterative solution for the 13 coefficients of (2) follows this ad hoc steepest descent procedure. Solutions were also found to be a function of which order the variables were searched. In this work and in K07, the search order was a, θ, x, and finally r_m. Variables were incremented up- and downgradient in the following order: c_2, c, γ, and finally v_m. Though we did not do a complete examination of the sensitivity to search order, we did examine a few other search orders, and solving for the asymmetries first provided larger asymmetries in the final solution and smaller errors overall. The first guess sets all coefficients to zero, except m_0 and x_0, which are initialized to the mean values of radius of maximum winds and the size parameter from the western North Pacific sample (34 n mi and 0.31). We did not use any other initial conditions. Following this initial step, we increment the coefficients in (2), one at a time, over a reasonable range of values (100 increments of 0.0005) to find the value of the minimum mean square error versus best track wind radii. This new minimum becomes the initial conditions for the next iteration. We repeat the search, moving up and down from the last minimum until we find convergence. Since the number of solutions to these equations is very large, we choose only the set of model coefficients that is physically consistent and near the global minimum in our loss function. Table 1 lists the final set of solutions. For comparison, Table 1 also lists the original coefficients from K07 (their Table 1), which were used in operations at JTWC, and the scaled versions from K07 (their Table 2).

The parametric vortex [(1)] with the parameters determined from the coefficients in Table 1 defines the climatological part of the CLIPER model. Note the larger constant for r_{mc} in the newly derived coefficients, and a much greater sensitivity of r_{mc} to both v_m and γ. The operational model from K07, on the other hand, has very little asymmetry (a_0–a_3) and a fixed r_{mc}. Because the r_{mc} is a function of latitude in the new model, TCs that are more intense and at higher latitude develop much larger circulations than either version of the coefficients given in K07. As a result, the new model should have larger asymmetries that are dependent on both latitude and storm speed, which is consistent with what we see in nature.

b. *Persistence*

Persistence is the second part of the model and is unchanged from what was done in K07—a process described briefly here. Tropical cyclones can have both symmetric and asymmetric differences from the

TABLE 1. Coefficients for (2) for the western North Pacific tropical cyclone basin used to create the climatological parametric wind radii CLIPER model. Coefficients from K07 [operational (their Table 1) and derived using the scaling method (their Table 2)], and the new version developed in this effort. Units for the coefficients are shown in the first column.

	Western Pacific (K07, Table 1) operational	Western Pacific (K07, Table 2) scaling method	Western Pacific (new)
t_0 (°)	15.0000	14.4000	−13.0300
t_1	−0.5500	−0.0288	0.8485
t_2 (° kt^{-1})	1.0200	1.8000	1.0653
a_o (kt)	0.6300	6.6800	4.2980
a_1	−0.0100	−0.1020	−0.1574
a_2 (kt^{-1})	0.0006	−0.0028	0.0035
a_3 (kt degree^{-1})	−0.0300	0.1620	0.1276
x_0	−0.0059	0.2355	0.3151
x_1 (kt^{-1})	0.0055	0.0039	0.0038
x_2 (degree^{-1})	−0.0031	−0.0028	−0.0022
m_0 (n mi)	20.0000	38.0000	56.9200
m_1 (n mi kt^{-1})	0.0000	−0.1167	−0.1541
m_2 (n mi degree^{-1})	0.0000	0.0000	0.7372

climatological model that can greatly influence the estimation of wind radii. Recall that the parameter x in our parametric model [(1)] represents the symmetric TC size. Using the observed wind radii and the climatological radius of maximum wind r_{mc}, a value of x (x_{obs}) that provides the best fit to the symmetric mean of the observed radii (e.g., the average of the northeast, southeast, southwest, and northwest quadrants) is computed. This is done for each of the 34-, 50-, and 64-kt wind radii. The difference between x_{obs} and x_c is then defined as the initial symmetric error.

Then, we use lag correlations of x_{obs} for the persistence. The lag correlations of the shape parameter x for our western North Pacific sample is shown in Fig. 1, where the points are the observed lag correlations, and the line is an approximation calculated as follows. First, we calculate the value of x_{obs} from the initial observations to capture the persistent nature of TC size. Then, we apply the 12-h basin-specific, linear regression coefficient and intercept to create a predicted value of x at 12 h:

$$x_{12} = x_c + [r_c(x_{\text{obs}} - x_c) + b_c]. \quad (3)$$

In (3), x_c is the climatological value of x calculated using the forecast position and intensity at $t = 12$ h, r_c is the regression coefficient, and b_c is the intercept. In this sample, $r_c = 0.71$ and $b_c = -0.01$ at $t = 12$ h. This calculation is repeated to estimate x at 24–120 h using the same values of r_c and b_c, where x_{obs} is replaced by the previous 12-h forecast. For example, the equation for 48 h is

$$x_{48} = x_c + [r_c(x_{36} - x_c) + b_c]. \quad (4)$$

In (4), x_c is the climatological value of x calculated using the 48-h forecast position and intensity. Instead of the observed x, we now use the 36-h x (x_{36}) in the equation for 48 h. This methodology approximates the points well, as shown in Fig. 1, but without the added complication of carrying nine additional coefficients and intercepts.

To compute the persistence of the asymmetric errors, we use the following strategy. First, initial wind radii estimates are again used to calculate x_{obs}. Then, x_{obs} is used in (1) to predict wind radii in each quadrant at $t = 0$. The differences between the predicted and observed wind radii in each quadrant are calculated and treated as initial errors in each of the observed wind radii. At $t = 0$ these errors are added back to the predicted values so that the observed wind radii match the predicted wind radii at $t = 0$. An e-folding time is used to phase out the persistence of the asymmetric errors, and as in K07 this e-folding time is set to 32 h. The initial errors effectively decay exponentially with time, becoming less than 5% of its initial value by 120 h.

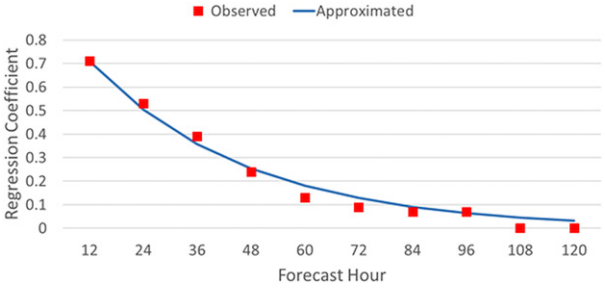

FIG. 1. Points represent the linear lag correlation coefficient for the relationship between the initial size parameter x and the observed x for each forecast hour. The curve is the approximation used by the parametric wind radii CLIPER model based on the 12-h intercept and lag correlation coefficient.

c. *Intensification*

If the storm intensifies past critical wind radii thresholds during the forecast, the model generates forecasts for wind radii for these higher wind speed thresholds. Initial errors from the next-lower wind radii threshold provide an estimate of the asymmetries for the higher-threshold wind radii. For instance, the initial R34 asymmetries for a storm that has maximum winds of 45 kt are used to add asymmetry to the predicted R50 when the TC is forecast to intensify to 50 kt. In this way, the higher-threshold wind radii asymmetries are prescribed to be consistent with R34 asymmetries throughout the intensification process, regardless of the initial intensity.

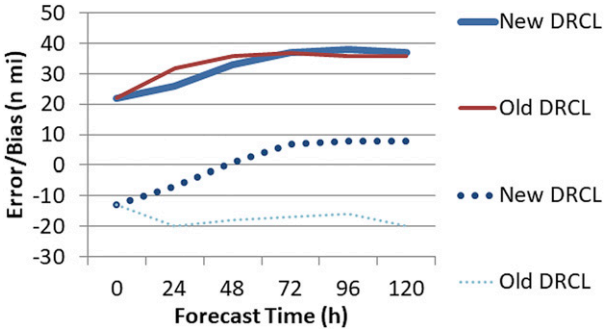

FIG. 2. Old and newly recomputed DRCL mean forecast errors (solid) and biases (dotted) for R34 using 2016 western North Pacific season JTWC best tracks as the baseline. Cases for $t = 0$, 24, 48, 72, 96, and 120 h are 1353, 1510, 1185, 861, 588, and 380, respectively.

3. Discussion

This work provides an update to the vortex climatology of the wind radii CLIPER model (ATCF technique named DRCL) for the western North Pacific. The original vortex climatology discussed in K07 was too small and too symmetric, resulting in unrealistically small wind radii. It is important to note that the DRCL model formulation has not changed and DRCL forecasts are still a blend of initial wind radii conditions and a climatological vortex that is a function of storm intensity, latitude, and the direction and speed of motion. JTWC forecasters provide both the initial wind radii and forecasts of future positions and intensities. The updated western North Pacific DRCL coefficients are developed with average radii that are 20%–35% larger than in the original operational model. As a result, the forecast wind radii for the longer ranges (after 48 h) are noticeably larger. The initial conditions provided by JTWC forecasters, however, will largely determine the 0–24-h forecasts of wind radii. Figure 2 shows a comparison of independent 2016 DRCL forecasts using the older K07 climatology and the updated climatology presented here. Figure 2 shows that the errors are similar, but the large negative biases in the older K07 climatology are eliminated by using this new climatology. R50 and R64 wind radii are purposely deemphasized here as the best track values are regressed from the subjectively determined R34 and intensity. It is felt that a higher quality validation dataset is required to properly derive and evaluate the R50 and R64 performance of this model. However, users should know that the new formulation generally results in larger R50 and R64 forecasts as well.

Beginning in 2014, a concerted effort involving several agencies was initiated to 1) determine the fidelity of wind radii estimation and forecasting and 2) develop tools and guidance to aid forecasters with the initial estimates and forecasts of tropical cyclone surface winds. Sampson et al. (2017), Sampson and Knaff (2015), and Knaff et al. (2017) describe many of these efforts. Because of this effort, operators and researchers should be aware that the JTWC wind radii are now generally larger, in both the best tracks and in the real-time estimates used to initialize NWP models and other applications. Prior to September 2017, the DRCL in operations at JTWC (developed in K07) was derived with the real-time wind radii estimates made with little objective guidance. The result was large negative wind radii biases at longer leads (as Fig. 2 shows for the 2016 western North Pacific season) and initial gale force wind radii forecasts (i.e., when the TC first exceeded 34 kt) that were inconsistent with new wind radii guidance. Note that $t = 0$ errors in Fig. 2 are the result of differences between wind radii used for initialization (i.e., real-time estimates) and the values in the final best tracks. The effort presented here and in prior work should address many of these inconsistencies. Furthermore, coefficients developed within this work will be used for the wind speed probability product (DeMaria et al. 2009, 2013) run using JTWC forecasts and, thus, should provide improvements to downstream products like TC conditions of readiness (Sampson et al. 2012) and significant wave-height probability forecasts (Sampson et al. 2016). Finally, the development of the DRCL model presented here can easily be extended to longer-lead forecasts, if JTWC extends their wind radii forecasts beyond 120 h.

Acknowledgments. This work was funded by the U.S. Navy under Contract N00604-16-P-3503 at the Cooperative Institute for Research in the Atmosphere and through the Office of Naval Research, Program Elements 0602435N. We would also like to thank the two

anonymous reviewer and the associate editor, Elizabeth Ritchie, for their comments and suggestions. The views, opinions, and findings contained in this report are those of the authors and should not be construed as an official National Oceanic and Atmospheric Administration or U.S. government position, policy, or decision.

REFERENCES

Debye, P., 1909: Näherungsformeln für die Zylinderfunktionen für große Werte des Arguments und unbeschränkt veränderliche Werte des Index (in German). *Math. Ann.*, **67**, 535–558, https://doi.org/10.1007%2FBF01450097.

DeMaria, M., J. A. Knaff, R. Knabb, C. Lauer, C. R. Sampson, and R. T. DeMaria, 2009: A new method for estimating tropical cyclone wind speed probabilities. *Wea. Forecasting*, **24**, 1573–1591, https://doi.org/10.1175/2009WAF2222286.1.

——, and Coauthors, 2013: Improvements to the operational tropical cyclone wind speed probability model. *Wea. Forecasting*, **28**, 586–602, https://doi.org/10.1175/WAF-D-12-00116.1.

Demuth, J., M. DeMaria, and J. A. Knaff, 2006: Improvement of Advanced Microwave Sounding Unit tropical cyclone intensity and size estimation algorithms. *J. Appl. Meteor. Climatol.*, **45**, 1573–1581, https://doi.org/10.1175/JAM2429.1.

Klotz, B. W., and H. Y. Jiang, 2016: Global composites of surface wind speeds in tropical cyclones based on a 12 year scatterometer database. *Geophys. Res. Lett.*, **43**, 10 480–10 488, https://doi.org/10.1002/2016GL071066.

Knaff, J. A., C. Guard, J. Kossin, T. Marchok, B. Sampson, T. Smith, and N. Surgi, 2007a: Operational guidance and skill in forecasting structure change. *Sixth Int. Workshop on Tropical Cyclones*, San José, Costa Rica, WMO Tech. Doc. 1383, http://severe.worldweather.org/iwtc/document.htm.

——, C. R. Sampson, M. DeMaria, T. P. Marchok, J. M. Gross, and C. J. McAdie, 2007b: Statistical tropical cyclone wind radii prediction using climatology and persistence. *Wea. Forecasting*, **22**, 781–791, https://doi.org/10.1175/WAF1026.1.

——, M. DeMaria, D. A. Molenar, C. R. Sampson, and M. G. Seybold, 2011: An automated, objective, multisatellite platform tropical cyclone surface wind analysis. *J. Appl. Meteor. Climatol.*, **50**, 2149–2166, https://doi.org/10.1175/2011JAMC2673.1.

——, S. P. Longmore, and D. A. Molenar, 2014: An objective satellite-based tropical cyclone size climatology. *J. Climate*, **27**, 455–476, https://doi.org/10.1175/JCLI-D-13-00096.1.

——, ——, R. T. DeMaria, and D. A. Molenar, 2015: Improved tropical-cyclone flight-level wind estimates using routine infrared satellite reconnaissance. *J. Appl. Meteor. Climatol.*, **54**, 463–478, https://doi.org/10.1175/JAMC-D-14-0112.1.

——, C. J. Slocum, K. D. Musgrave, C. R. Sampson, and B. R. Strahl, 2016: Using routinely available information to estimate tropical cyclone wind structure. *Mon. Wea. Rev.*, **144**, 1233–1247, https://doi.org/10.1175/MWR-D-15-0267.1.

——, C. R. Sampson, and G. Chirokova, 2017: A global statistical–dynamical tropical cyclone wind radii forecast scheme. *Wea. Forecasting*, **32**, 629–644, https://doi.org/10.1175/WAF-D-16-0168.1.

Merrill, R. T., 1984: A comparison of large and small tropical cyclones. *Mon. Wea. Rev.*, **112**, 1408–1418, https://doi.org/10.1175/1520-0493(1984)112<1408:ACOLAS>2.0.CO;2.

Sampson, C. R., and A. J. Schrader, 2000: The Automated Tropical Cyclone Forecasting system (version 3.2). *Bull. Amer. Meteor. Soc.*, **81**, 1231–1240, https://doi.org/10.1175/1520-0477(2000)081<1231:TATCFS>2.3.CO;2.

——, and J. A. Knaff, 2015: A consensus forecast for tropical cyclone gale wind radii. *Wea. Forecasting*, **30**, 1397–1403, https://doi.org/10.1175/WAF-D-15-0009.1.

——, and Coauthors, 2012: Objective guidance for use in setting tropical cyclone conditions of readiness. *Wea. Forecasting*, **27**, 1052–1060, https://doi.org/10.1175/WAF-D-12-00008.1.

——, J. A. Hansen, P. A. Wittmann, J. A. Knaff, and A. Schumacher, 2016: Wave probabilities consistent with official tropical cyclone forecasts. *Wea. Forecasting*, **31**, 2035–2045, https://doi.org/10.1175/WAF-D-15-0093.1.

——, E. M. Fukada, J. A. Knaff, B. R. Strahl, M. J. Brennan, and T. Marchok, 2017: Tropical cyclone gale wind radii estimates for the western North Pacific. *Wea. Forecasting*, **32**, 1029–1040, https://doi.org/10.1175/WAF-D-16-0196.1.

Uhlhorn, E. W., B. W. Klotz, T. Vukicevic, P. D. Reasor, and R. F. Rogers, 2014: Observed hurricane wind speed asymmetries and relationships to motion and environmental shear. *Mon. Wea. Rev.*, **142**, 1290–1311, https://doi.org/10.1175/MWR-D-13-00249.1.

Weatherford, C. L., and W. M. Gray, 1988: Typhoon structure as revealed by aircraft reconnaissance. Part II. Structural variability. *Mon. Wea. Rev.*, **116**, 1044–1056, https://doi.org/10.1175/1520-0493(1988)116<1044:TSARBA>2.0.CO;2.